第37卷第6期 2021年6月
无 机 化 学 学 报
CHINESE JOURNAL OF INORGANIC CHEMISTRY
Vol.37 No.6 1135-1142

由2,3-二羟基-对苯二甲酸配体构筑的锰(Ⅱ)和镉(Ⅱ)配位聚合物的合成、晶体结构、荧光及催化性质

黎 彧[#] 庄映芬[#] 张艳来 冯安生 邹训重*
(广东轻工职业技术学院,广东省特种建筑材料及其绿色制备工程技术研究中心/
佛山市特种功能性建筑材料及其绿色制备技术工程中心,广州 510300)

摘要: 采用水热方法,用2,3-二羟基-对苯二甲酸配体(H_4DTA)和2,2′-联吡啶(bipy)分别与$MnCl_2·4H_2O$和$CdCl_2·H_2O$反应,合成了2个三维配位聚合物$[M(\mu_4\text{-}H_2DTA)(bipy)]_n$(M=Mn (**1**)、Cd (**2**)),并对其结构、荧光和催化性质进行了研究。单晶结构分析结果表明2个配合物同构,均属于正交晶系,*Pnna*空间群。配合物**1**和**2**都具有三维框架结构。另外,研究了2个配合物的荧光和催化性质。研究表明,配合物**1**在硅腈化反应中表现出较高的催化活性。

关键词: 配位聚合物; 2,3-二羟基-对苯二甲酸; 荧光; 催化
中图分类号: O614.71$^+$1; O614.24$^+$2 **文献标识码:** A **文章编号:** 1001-4861(2021)06-1135-08
DOI: 10.11862/CJIC.2021.132

Syntheses, Crystal Structures, Luminescence and Catalytic Activity of Manganese(Ⅱ) and Cadmium(Ⅱ) Coordination Polymers Based on 2,3-Dihydroxy-terephthalic Acid

LI Yu[#] ZHUANG Ying-Fen[#] ZHANG Yan-Lai FENG An-Sheng ZOU Xun-Zhong*
(*Guangdong Research Center for Special Building Materials and Its Green Preparation Technology/ Foshan Research Center for Special Functional Building Materials and Its Green Preparation Technology, Guangdong Industry Polytechnic, Guangzhou* 510300, *China*)

Abstract: Two 3D manganese(Ⅱ) and cadmium(Ⅱ) coordination polymers, namely $[M(\mu_4\text{-}H_2DTA)(bipy)]_n$ (M=Mn (**1**), Cd (**2**)), have been constructed hydrothermally using H_4DTA (H_4DTA=2,3-dihydroxy-terephthalic acid), bipy (bipy= 2,2′-bipyridine), and manganese or cadmium chlorides. Single-crystal X-ray diffraction analyses reveal that two complexes are isostructural and crystallize in the orthorhombic system, space groups *Pnna*. Both complexes disclose a 3D metal-organic framework. The luminescent and catalytic properties of two complexes were investigated. Complex **1** exhibited good catalytic performance for the cyanosilylation reaction. CCDC: 2060258, **1**; 2060259, **2**.

Keywords: coordination polymer; 2,3-dihydroxy-terephthalic acid; luminescence; catalytic

0 Introduction

The design of functional coordination polymers (CPs) turned to be a hot research topic[1-3], especially considering a huge diversity of potential applications of such complexes and derived materials in gas storage and separation[4-6], catalysis[7-10], molecular magnetism[11-12], photochemistry[13-15], and selective sensing[16-18]. Although the assembly of CPs may depend on many parameters (*e. g.*, types of metal ions[10-11], linkers[16,18], supporting ligands[19-20], solvent[21-22], molar

收稿日期:2021-02-02。收修改稿日期:2021-03-25。
广州市科技计划项目(No.201904010381,201804010499)和广东省教育厅青年人才项目(No.2018GkQNCX033)资助。
[#]共同第一作者。
*通信联系人。E-mail:2017018009@gdip.edu.cn

ratios of reagents[23-25] and temperature conditions[26-27]), the nature of metal ions and organic linkers are undoubtedly the key factors that usually define the structures and functional properties of the obtained complexes. Aromatic carboxylic acids containing several COOH functionalities represent the most populated family of linkers in the research on CPs, especially given their availability and reasonable cost, thermal stability, possibility of further functionalization and multitude of coordination modes[22-23,28-29].

In particular, terephthalic acid is one of the simplest and common building blocks that is widely used for the synthesis of different CPs and MOFs (metal-organic frameworks)[30-33]. However, the functionalized terephthalate ligands remain significantly less investigated[30]. For example, an introduction of two hydroxy substituents into terephthalic acid may well affect its coordination behavior and structures of the resulting complexes. Given an unexplored coordination chemistry of 2, 3-dihydroxy-terephthalic acid[34-35], the main aim of the present work consisted in widening the family of metal(Ⅱ) coordination polymers with this dicarboxylate linker and searching for potential catalytic applications of the obtained complexes.

Herein, we report the syntheses, crystal structures, luminescent and catalytic properties of two Mn(Ⅱ) and Cd(Ⅱ) coordination polymers constructed from the 2,3-dihydroxy-terephthalic acid.

1 Experimental

1.1 Reagents and physical measurements

All chemicals and solvents were of AR grade and used without further purification. Carbon, hydrogen and nitrogen were determined using an Elementar Vario EL elemental analyzer. IR spectrum was recorded using KBr pellets and a Bruker EQUINOX 55 spectrometer. Thermogravimetric analysis (TGA) data were collected on a LINSEIS STA PT1600 thermal analyzer with a heating rate of 10 ℃·min^{-1}. Powder X-ray diffraction patterns (PXRD) were measured on a Rigaku-Dmax 2400 diffractometer using Cu $K\alpha$ radiation (λ = 0.154 06 nm). The X-ray tube was operated at 40 kV and 40 mA, and the data collection range was between 5° and 45°. Excitation and emission spectra were recorded on an Edinburgh FLS920 fluorescence spectrometer using the solid samples at room temperature. Solution ^{1}H NMR spectra were recorded on a JNM ECS 400M spectrometer.

1.2 Syntheses of [M(μ_4-H_2DTA)(bipy)]$_n$ (M=Mn (1) and Cd (2))

A mixture of $MCl_2 \cdot xH_2O$ (x=4 for **1** and x=1 for **2**; 0.20 mmol), H_4DTA (0.040 g, 0.20 mmol), bipy (0.031 g, 0.20 mmol), NaOH (0.016 g, 0.40 mmol), and H_2O (10 mL) was stirred at room temperature for 15 min, and then sealed in a 25 mL Teflon-lined stainless steel vessel, and heated at 160 ℃ for 3 days, followed by cooling to room temperature at a rate of 10 ℃·h^{-1}. Yellow (**1**) or colourless (**2**) block-shaped crystals were isolated manually, and washed with distilled water. Yield: 51% for **1** and 42% for **2** (based on H_4DTA). Anal. Calcd. for $C_{18}H_{12}MnN_2O_6$ (**1**, %): C 53.09, H 2.97, N 6.88; Found(%): C 53.01, H 2.99, N 6.83. IR (KBr, cm^{-1}): 1 638w, 1 594s, 1 474m, 1 441m, 1 388s, 1 330m, 1 260m, 1 222w, 1 132w, 1 062w, 1 013w, 852w, 835w, 810m, 764m, 736w, 646w. Anal. Calcd. for $C_{18}H_{12}CdN_2O_6$ (2, %): C 46.52, H 2.60, N 6.03; Found (%): C 46.41, H 2.58, N 6.06. IR (KBr, cm^{-1}): 1 631w, 1 594s, 1 474m, 1 441m, 1 383s, 1 330m, 1 251m, 1 222w, 1 132w, 1 062w, 1 013w, 860w, 811m, 770m, 736w, 649w.

The complexes are insoluble in water and common organic solvents, such as methanol, ethanol, acetone and DMF.

1.3 Structure determination

Two single crystals with dimensions of 0.25 mm×0.23 mm×0.22 mm (**1**) and 0.23 mm×0.22 mm×0.21 mm (**2**) were collected at 293(2) K on a Bruker SMART APEX Ⅱ CCD diffractometer with Cu $K\alpha$ radiation (λ = 0.154 178 nm). The structures were solved by direct methods and refined by full matrix least-square on F^2 using the SHELXTL-2014 program[36]. All non-hydrogen atoms were refined anisotropically. All the hydrogen atoms were positioned geometrically and refined using a riding model. A summary of the crystallography data and structure refinements for **1** and **2** is given in Table 1. The selected bond lengths and angles for complexes **1** and **2** are listed in Table 2.

Table 1　Crystal data for complexes 1 and 2

Complex	1	2
Chemical formula	$C_{18}H_{12}MnN_2O_6$	$C_{18}H_{12}CdN_2O_6$
Molecular weight	407.24	464.70
Crystal system	Orthorhombic	Orthorhombic
Space group	*Pnna*	*Pnna*
a / nm	0.964 95(4)	0.976 18(3)
b / nm	1.692 31(8)	1.685 18(4)
c / nm	1.024 19(5)	1.042 57(3)
V / nm^3	1.672 51(13)	1.715 06(9)
Z	4	4
F(000)	828	920
θ range for data collection / (°)	5.048~69.827	4.988~66.524
Limiting indices	$-11 \leqslant h \leqslant 9$, $-20 \leqslant k \leqslant 18$, $-7 \leqslant l \leqslant 12$	$-7 \leqslant h \leqslant 11$, $-20 \leqslant k \leqslant 18$, $-12 \leqslant l \leqslant 10$
Reflection collected, unique (R_{int})	5 632, 1 573 (0.068 9)	5 351, 1 494 (0.042 2)
D_c / (g·cm^{-3})	1.617	1.800
μ / mm^{-1}	6.791	10.564
Data, restraint, parameter	1 573, 0, 124	1 494, 0, 124
Goodness-of-fit on F^2	1.049	1.021
Final R indices [$I \geqslant 2\sigma(I)$] R_1, wR_2	0.046 7, 0.097 9	0.047 5, 0.120 4
R indices (all data) R_1, wR_2	0.084 9, 0.107 5	0.051 8, 0.127 3
Largest diff. peak and hole / (e·nm^{-3})	333 and −433	929 and −3 169

Table 2　Selected bond distances (nm) and bond angles (°) for complexes 1 and 2

		1			
Mn1—O1	0.213 7(2)	Mn1—O1B	0.213 7(2)	Mn1—O2C	0.217 8(2)
Mn1—O2D	0.217 8(2)	Mn1—N1	0.229 8(3)	Mn1—N1B	0.229 8(3)
O1—Mn1—O1B	164.71(15)	O2D—Mn1—O1B	90.39(9)	O2D—Mn1—O1	80.50(9)
O2D—Mn1—O2C	106.99(14)	O1—Mn1—N1	93.79(11)	O1—Mn1—N1B	98.68(10)
O2C—Mn1—N1	91.57(11)	O2D—Mn1—N1	160.51(11)	N1—Mn1—N1B	70.75(16)
		2			
Cd1—O1	0.225 6(2)	Cd1—O1B	0.225 6(2)	Cd1—O2C	0.228 8(2)
Cd1—O2D	0.228 8(2)	Cd1—N1	0.234 9(3)	Cd1—N1B	0.234 9(3)
O1—Cd1—O1B	107.74(17)	O2D—Cd1—O1B	89.25(10)	O2D—Cd1—O1	75.84(9)
O2D—Cd1—O2C	154.75(14)	O1—Cd1—N1	91.97(12)	O1—Cd1—N1B	158.64(11)
O2C—Cd1—N1	96.81(11)	O2D—Cd1—N1	103.85(11)	N1—Cd1—N1B	70.04(16)

Symmetry codes: B: $-x+1/2, -y+1, z$; C: $x+1/2, y, -z+1$; D: $-x, -y+1, -z+1$ for **1**; B: $-x+1/2, -y+1, z$; C: $x+1/2, y, -z+1$; D: $-x, -y+1, -z+1$ for **2**.

CCDC: 2060258, **1**; 2060259, **2**.

1.4　Catalytic cyanosilylation of aldehydes

In a typical test, a suspension of an aromatic aldehyde (0.50 mmol, 4-nitrobenzaldehyde as a model substrate), trimethylsilyl cyanide (1.0 mmol) and the catalyst (typically, molar fraction=3%) in dichloromethane (2.5 mL) was stirred at 35 ℃. After a desired reaction time, the catalyst was removed by centrifugation, followed by an evaporation of the solvent from the filtrate under reduced pressure to give a crude solid. This was dissolved in $CDCl_3$ and analyzed by ^{1}H NMR spectroscopy for quantification of products (Fig.S1). To perform

the recycling experiment, the catalyst was isolated by centrifugation, washed with dichloromethane, dried at room temperature, and reused. The subsequent steps were performed as described above.

2 Results and discussion

2.1 Description of structure of 1 and 2

Complexes **1** and **2** are isostructural (Table 1) and the structure of **1** is discussed in detail as an example. Complex **1** reveals a 3D metal-organic framework with the asymmetric unit containing a Mn(Ⅱ) ion (with half occupancy), a half of μ_4-H_2DTA^{2-} ligand, and a half of bipy moiety. The Mn(Ⅱ) center is six-coordinated and reveals a octahedral $\{MnN_2O_4\}$ environment, which is completed by four carboxylate O atoms from four individual μ_4-H_2DTA^{2-} blocks and a pair of N atoms from the bipy moiety (Fig. 1). The lengths of Mn—O and Mn—N bonds are 0.213 7(3)~0.217 8(3) nm and 0.229 8(3) nm, respectively; these are within the normal values for related Mn(Ⅱ) derivatives[11,22,27]. The H_2DTA^{2-} block acts as a μ_4-linker via bidentate COO^- groups (Scheme 1). The intramolecular hydrogen bond (O3—H3···O2) was found. The μ_4-H_2DTA^{2-} blocks connect adjacent Mn1 ions to form a 3D metal-organic framework (Fig.2). This crystal structure features an intricate 3D metal-organic net that is built from the 4-connected, topologically distinct Mn1 and μ_4-H_2DTA^{2-} nodes (Fig.3). The resulting net can be classified as a

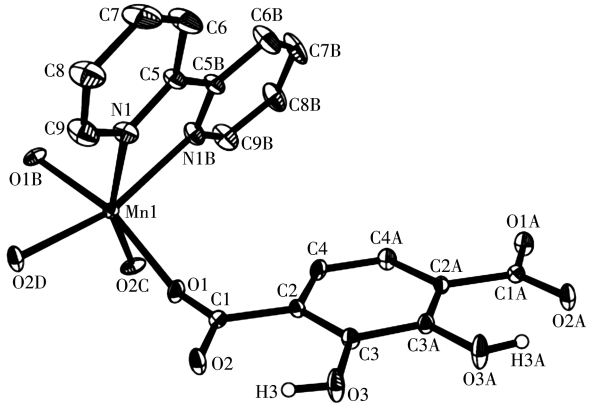

Hydrogen atoms are omitted for clarity except those bonding to oxygen atoms; Symmetry codes: A: x, $-y+1/2$, $-z+3/2$; B: $-x+1/2$, $-y+1$, z; C: $x+1/2$, y, $-z+1$; D: $-x$, $-y+1$, $-z+1$

Fig.1 Drawing of coordination environment around Mn(Ⅱ) center in complex **1** with 30% probability thermal ellipsoids

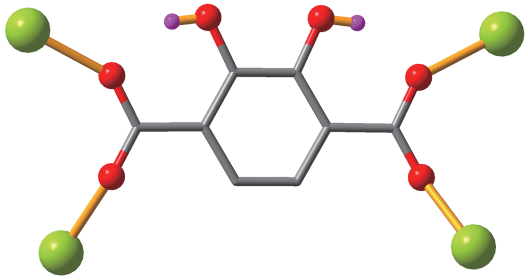

Scheme 1 Coordination mode of H_2DTA^{2-} ligand in complex **1**

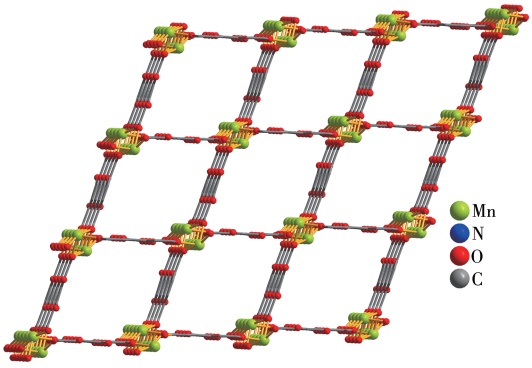

Bipy ligands are omitted for clarity

Fig.2 Perspective of 3D metal-organic framework along a axis

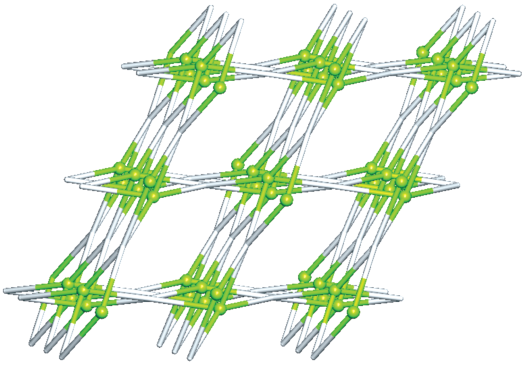

Green balls: 4-connected Mn1, Gray: centroids of 4-connected μ_4-H_2DTA^{2-} nodes

Fig.3 Topological representation of binodal 4,4-connected metal-organic framework with a *pts* topology viewed along a axis

binodal 4,4-connected framework with a *pts* (PtS, cooperate) topology and point symbol of $(4^2.8^4)$.

2.2 TGA analysis

To determine the thermal stability of complexes **1** and **2**, their thermal behaviors were investigated under nitrogen atmosphere by TGA. As shown in Fig.4, both complexes did not contain solvent of crystallization or

H_2O ligands and remains stable up to 305 and 282 ℃, respectively, followed by a decomposition on further heating.

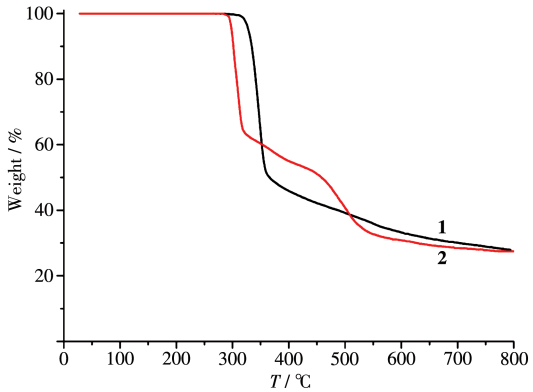

Fig.4　TGA curves of complexes **1** and **2**

2.3　Luminescent properties

Solid-state emission spectra of H_4DTA and complex **2** were measured at room temperature (Fig.5). The spectrum of H_4DTA revealed a weak emission with a maximum at 426 nm (λ_{ex}=310 nm). In comparison with H_4DTA, complex **2** exhibited a more extensive emission at 388 nm (λ_{ex}=310 nm). These emissions correspond to intraligand π - π^* or n - π^* transition of H_4DTA[11,22-23]. Enhancement of the luminescence in **2** compared to H_4DTA can be explained by the coordination of ligands to Cd(Ⅱ); the coordination can augment a rigidity of ligand and reduce an energy loss due to radiationless decay[22-23,37].

2.4　Catalytic cyanosilylation of aldehydes

Given the potential of Mn(Ⅱ) and Cd(Ⅱ) complexes to catalyze the organic reactions[38-40], we explored the application of **1** and **2** as heterogeneous catalysts in the

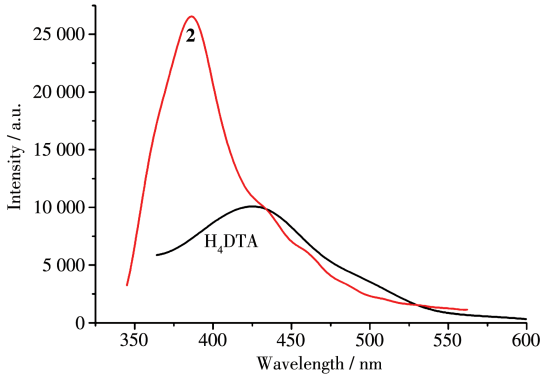

Fig.5　Solid-state emission spectra of H_4DTA and complex **2** at room temperature

cyanosilylation of 4-nitrobenzaldehyde as a model substrate to give 2-(4-nitrophenyl)-2-((trimethylsilyl)oxy) acetonitrile. Typical tests were carried out by reacting a mixture of 4-nitrobenzaldehyde, trimethylsilyl cyanide (TMSCN), and the catalyst in dichloromethane at 35 ℃ (Scheme 2, Table 3). Such effects as reaction time, catalyst loading, solvent composition, catalyst recycling and finally substrate scope were investigated.

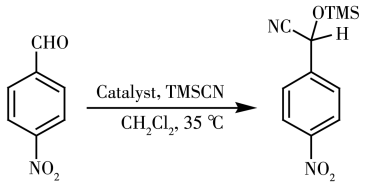

Scheme 2　Catalyzed cyanosilylation of 4-nitrobenzaldehyde (model substrate)

Upon using complex **1** as the catalyst (Molar fraction: 3%), a high conversion of 93% of 4-nitrobenzaldehyde into 2-(4-nitrophenyl)-2-((trimethylsilyl)oxy)acetonitrile was reached after 12 h in dichloromethane at 35 ℃ (Table 3, Entry 7). Upon extending the reaction time further to 18 h, only a slight increase in the product yield to 94% occurred. Moreover, no other products were detected, and the yield of this product was considered to be the conversion of 4-nitrobenzaldehyde (Fig.6).

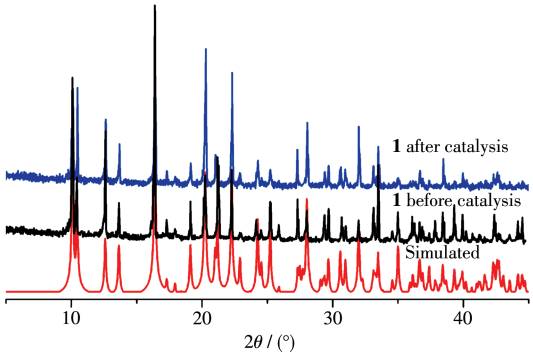

Fig.6　PXRD patterns for **1**: simulated (red), before (black) and after (blue) catalysis

We also compared the activities of catalyst **1** in the reactions of other substituted aromatic and aliphatic aldehydes with trimethylsilyl cyanide, and the corresponding cyanohydrin derivatives were produced in yields ranging from 48% to 93% (Table 4). Aryl aldehydes bearing strong electron-withdrawing substituents

Table 3 Catalyzed cyanosilylation of 4-nitrobenzaldehyde with TMSCN

Entry	Catalyst	Time / h	Catalyst dosage[a] / %	Solvent	Yield[b] / %
1	1	1	3.0	CH_2Cl_2	33
2	1	2	3.0	CH_2Cl_2	60
3	1	4	3.0	CH_2Cl_2	70
4	1	6	3.0	CH_2Cl_2	78
5	1	8	3.0	CH_2Cl_2	85
6	1	10	3.0	CH_2Cl_2	88
7	1	12	3.0	CH_2Cl_2	93
8	2	12	3.0	CH_2Cl_2	35
9	1	12	2.0	CH_2Cl_2	72
10	1	12	4.0	CH_2Cl_2	94
11	1	12	3.0	CH_3CN	81
12	1	12	3.0	THF	71
13	1	12	3.0	CH_3OH	85
14	1	12	3.0	CH_3Cl	87
15	Blank	12	—	CH_2Cl_2	5
16	$MnCl_2$	12	3.0	CH_2Cl_2	9
17	$CdCl_2$	12	3.0	CH_2Cl_2	6
18	H_3dpna	12	3.0	CH_2Cl_2	7

[a] Molar fraction; [b] Calculated by ^{1}H NMR spectroscopy: $n_{product}/n_{aldehyde}\times100\%$.

Table 4 Cyanosilylation of various aldehydes with TMSCN catalyzed by 1[a]

Entry	Substituted benzaldehyde substrate (R—C_6H_4CHO)	Product yield[b] / %
1	R=H	60
2	R=2-NO_2	81
3	R=3-NO_2	88
4	R=4-NO_2	93
5	R=4-Cl	63
6	R=4-OH	54
7	P=4-CH_3	48

[a] Reaction conditions: aldehyde (0.5 mmol), TMSCN (1.0 mmol), catalyst **1** (Molar fraction: 3.0%) and CH_2Cl_2 (2.5 mL) at 35 ℃; [b] Calculated by ^{1}H NMR spectroscopy.

(*e.g.*, nitro and chloro) exhibited the higher reactivities (Table 4, Entries 2~5), which may be related to an increase in the electrophilicity of the substrate. Aldehydes containing electron-donating proups (*e.g.*, methyl) showed lower reaction yields (Table 4, Entry 7) as expected. An *ortho*-substituted aldehyde showed lower reactivity, possibly as a result of steric hindrance.

To examine the stability of **1** in the cyanosilylation reaction, we tested the recyclability of this heterogeneous catalyst. For this purpose, upon completion of a reaction cycle, we separated the catalyst by centrifugation, washed it with CH_2Cl_2, and dried it at room temperature before its further use. We repeated recycling catalyst **1** and the catalytic system mained the higher activity over at least five consecutive cycles (the yields were 92%, 91%, 89% and 88% for second to fifth run, respectively). According to the PXRD data (Fig. 6), the structure of **1** was essentially preserved after five catalytic cycles.

A possible catalytic cycle for the cyanosilylation reaction catalyzed by a Mn coordination polymer is proposed in Scheme 3. It can involve dual activation of the carbonyl and TMSCN by the Mn(Ⅱ) centre and a ligated carboxylate group, respectively, followedby the forma-

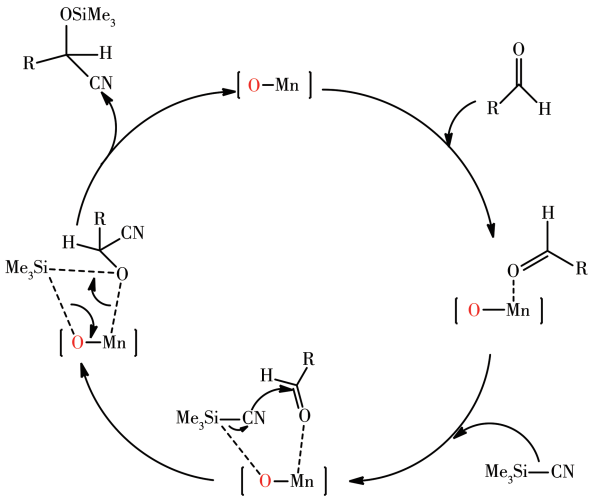

Scheme 3　Mechanism for Mn-catalyzed cyanosilylation reaction

tion of C—C bond leading to cyanohydrin[41-42].

3　Conclusions

In summary, we have successfully synthesized and characterized two new manganese and cadmium complexes by using one unexplored dicarboxylic acid as ligand under hydrothermal condition. Both complexes feature a 3D metal-organic framework structure. Besides, the luminescence and catalytic properties were also investigated and discussed. The results show that complex **1** exhibits a higher catalytic activity in the cyanosilylation at 35 ℃.

Supporting information is available at http://www.wjhxxb.cn

References:

[1] Batten S R, Neville S M, Turner D R. *Coordination Polymers: Design, Analysis and Application*. Cambridge: Royal Society of Chemistry, **2009**.

[2] Morsali A, Hashemi L. *Main Group Metal Coordination Polymers: Structures and Nanostructures*. Hoboken: John Wiley & Sons, Inc., **2017**.

[3] Pettinari C, Tăbăcaru A, Galli S. *Coord. Chem. Rev.*, **2016**,**307**:1-31

[4] Cheng F J, Li Q Q, Duan J G, Hosono N, Noro S , Krishna R, Lyu H L, Kusaka S, Jin W Q, Kitagawa S. *J. Mater. Chem. A*, **2017**,**5**(34): 17874-17880

[5] Fan W D, Wang X, Xu B, Wang Y T, Liu D D, Zhang M, Shang Y Z, Dai F N, Zhang L L, Sun D F. *J. Mater. Chem. A*, **2018**,**6**(47):24486-24495

[6] Zheng B S, Luo X, Wang Z X, Zhang S W, Yun R R, Huang L, Zeng W J, Liu W L. *Inorg. Chem. Front.*, **2018**,**5**(9):2355-2363

[7] Du Y, Yang H S, Wan S, Jin Y H, Zhang W. *J. Mater. Chem. A*, **2017**, **5**(19):9163-9168

[8] Gu J Z, Wen M, Cai Y, Shi Z F, Nesterov D S, Kirillova M V, Kirillov A M. *Inorg. Chem.*, **2019**,**58**(9):5875-5885

[9] Gu J Z, Wen M, Cai Y, Shi Z F, Arol A S, Kirillova M V, Kirillov A M. *Inorg. Chem.*, **2019**,**58**(4):2403-2412

[10]Fernandes T A, Santos C I M, André V, Klak J, Kirillova M V, Kirillov A M. *Inorg. Chem.*, **2016**,**55**(1):125-135

[11]Gu J Z, Liang X X, Cai Y, Wu J, Shi Z F, Kirillov A M. *Dalton Trans.*, **2017**,**46**(33):10908-10925

[12]Karabach Y Y, Kirillov A M, Haukka M, Sanchiz J, Kopylovich M N, Pombeiro A J L. *Cryst. Growth Des.*, **2008**,**8**(11):4100-4108

[13]Zhao J, Liu B A, Feng Z, Jin D Y, Dang W P, Yang X L, Zhou G J, Wu Z X, Wong W Y. *Polym. Chem.*, **2017**,**8**(41):6368-6377

[14]Einkauf J D, Clark J M, Paulive A, Tanner G P, de Lill D T. *Inorg. Chem.*, **2017**,**56**(10):5544-5552

[15]Hasegawa Y, Miura Y, Kitagawa Y, Wada S, Nakanishi T, Fushimi K, Seki T, Ito H, Iwasa T, Taketsugu T, Gon M, Tanaka K, Chujo Y, Hattori S, Karasawa M, Ishii K. *Chem. Commun.*, **2018**,**54**(76):10695-10697

[16]Mayhugh J T, Niklas J E, Forbes M G, Gorden J D, Gorden A E V. *Inorg. Chem.*, **2020**,**59**(14):9560-9568

[17]Haldar R, Matsuda R, Kitagawa S, George S J, Maji T K. *Angew. Chem. Int. Ed.*, **2014**,**53**(44):11772-11777

[18]Jaros S W, Sokolnicki J, Woloszyn A, Haukka M, Kirillov A M, Smoleński P. *J. Mater. Chem. C*, **2018**,**6**(7):1670-1678

[19]Wei N, Zhang M Y, Zhang X N, Li G M, Zhang X D. *Cryst. Growth Des.*, **2014**,**14**(6):3002-3009

[20]Bosch M, Sun X, Yuan S, Chen Y P, Wang Q, Wang X, Zhou H C. *Eur. J. Inorg. Chem.*, **2016**(27):4368-4372

[21]Kühne I A, Carter A B, Kostakis G E, Anson C E, Powell A K. *Crystals*, **2020**,**10**:893

[22]Gu J Z, Gao Z Q, Tang Y. *Cryst. Growth Des.*, **2012**,**12**(6):3312-3323

[23]Gu J Z, Cui Y H, Wu J, Kirillov A M. *RSC Adv.*, **2015**,**5**(96):78889-78901

[24]Ye R P, Zhang X, Zhang L, Zhang J, Yao Y G. *Cryst. Growth Des.*, **2016**,**16**(7):4012-4020

[25]Hou X Y, Wang X, Li S N, Jiang Y C, Hou M C. *Cryst. Growth Des.*, **2017**,**17**(6):3229-3235

[26]邹训重, 吴疆, 顾金忠, 赵娜, 冯安生, 黎彧. 无机化学学报, **2019**, **35**(9):1705-1711
ZOU X Z, WU J, GU J Z, ZHAO N, FENG A S, LI Y. *Chinese J. Inorg. Chem.*, **2019**,**35**(9):1705-1711

[27]Li Y, Wu J, Gu J Z, Qiu W D, Feng A S. *Chin. J. Struct. Chem.*, **2020**,**39**(4):727-736

[28]Arici M, Yeşilel O Z, Taş M, Demiral H. *Cryst. Growth Des.*, **2017**,**17**(5):2654-2659

[29]Gu J Z, Wen M, Liang X X, Shi Z F, Kirillova M V, Kirillov A M. *Crystals*, **2018**,**8**:83

[30]Groom C R, Bruno I J, Lightfoot M P, Ward S C. *Acta Crystallogr. Sect. B*, **2016**,**B72**(2):171-179

[31]Logan M W, Lau Y A, Zheng Y, Hall E A, Hettinger M A, Marks R P, Hosler M L, Rossi F M, Yuan Y, Uribe-Romo F J. *Catal. Sci. Technol.*, **2016**,**6**(14):5647-5655

[32]Mian M R, Afrin U, Fataftah M S, Idrees K B, Islamoglu T, Freedman D E, Farha O K. *Inorg. Chem.*, **2020**,**59**(12):8444-8450

[33]Kim S N, Lee Y R, Hong S H, Jang M S, Ahn W S. *Catal. Today*, **2015**,**245**:54-60

[34]Lee H G, Jo H, Eom S, Kang D W, Kang M J, Hilgar J, Rinehart J D, Moon D, Hong C S. *Cryst. Growth Des.*, **2018**,**18**(6):3360-3365

[35]Fei H, Shin J, Meng Y S, Adelhardt M, Sutter J, Meyer K, Cohen S M. *J. Am. Chem. Soc.*, **2014**,**136**(13):4965-4973

[36]Spek A L. *Acta Crystallogr. Sect. C*, **2015**,**C71**(1):9-18

[37]Gu J Z, Cui Y H, Liang X X, Wu J, Lv D Y, Kirillov A M. *Cryst. Growth Des.*, **2016**,**16**(8):4658-4670

[38]Pal S, Maiti S, Nayek H P. *Appl. Organomet. Chem.*, **2018**,**32**:e4447

[39]Loukopoulos E, Kostakis G E. *J. Coord. Chem.*, **2018**,**71**(3):371-410

[40]Hu L, Hao G X, Luo H D, Ke C X, Shi G, Lin J, Lin X M, Qazi U Y, Cai Y P. *Cryst. Growth Des.*, **2018**,**18**(5):2883-2889

[41]Karmakar A, Hazra S, da Silva M F C G, Pombeiro A J L. *Dalton Trans.*, **2015**,**44**(1):268-280

[42]Aguirre-Díaz L M, Iglesias M, Snejko N, Gutiérrez-Puebla E, Monge M Á. *CrystEngComm*, **2013**,**15**(45):9562-9571